

Indicators for cluster survivability in a dispersing cloud

Hui-Chen Chen¹ and Chung-Ming Ko^{1,2}

Institute of Astronomy, National Central University, Jhongli 320, Taiwan

ABSTRACT

We use N-body simulations to survey the response of embedded star clusters to the dispersal of their parent molecular cloud. The final stages of the clusters can be divided into three classes: the cluster (i) is destroyed, (ii) has a loose structure, and (iii) has a compact core. We are interested in three of the governing parameters of the parent cloud: (i) the mass, (ii) the size, and (iii) the dispersing rate. It is known that the final stage of the cluster is well correlated with the star formation efficiency (SFE) for systems with the same cluster and cloud profile. We deem that the SFE alone is not enough to address systems with clouds of different sizes. Our result shows that the initial cluster-cloud mass ratio at a certain Lagrangian radius, and the initial kinetic energy are better indicators for the survivability of embedded clusters.

Subject headings: methods: *N*-body simulations - open clusters and associations: general - galaxies: star clusters

1. Introduction

Stars are the fundamental units to build up a galaxy and are mostly not born alone but in groups. Stellar groups, clusters, or associations are formed inside molecular clouds. They are embedded and not optically seen until they get rid of the residual material after star formation. An embedded cluster is not always understood clearly because of observational constraints. The near-infrared all sky survey, Two Micron All Sky Survey, has given astronomers a chance to look into the clouds. Lada & Lada (2003) claimed that the number of embedded clusters declines rapidly with age and the infant mortality of clusters (i.e., disruption not long after birth) is more than 90% in our Galaxy.

¹Institute of Astronomy, National Central University, Jhongli 320, Taiwan

²Department of Physics and Center for Complex Systems, National Central University, Jhongli 320, Taiwan

Galactic tidal forces, close encounters with giant molecular clouds (Gieles et al. 2006), shock heating, and mass loss of the system by massive member stars, such as UV radiation, stellar winds, and supernova explosions (Boily & Kroupa 2003a,b), are possible disruption mechanisms for stellar groups, whether they are embedded or not. Nonetheless, most of these mechanisms (such as the first three aforementioned mechanisms) have a destruction timescale longer than the upper limit of the lifetime of molecular clouds, which is about a few to a few tens of Myr (Blitz & Shu 1980; Elmegreen 2000; Hartmann et al. 2001; Bonnell et al. 2006). CO observations in our Galaxy suggested that the lifetime of molecular clouds is of the order of 10 Myr (Leisawitz et al. 1989). Timescale estimation of photoevaporation and statistics on the expected numbers of stars per cloud showed that giant molecular clouds of mass $10^6 M_\odot$ are expected to survive for about 30 Myr (Williams & McKee 1997). The most promising disruption mechanism for embedded clusters seems to be the dispersion of the parent cloud by UV radiation, stellar winds, and supernova explosions in early cluster evolution (see, e.g., Tutukov 1978; Lada et al. 1984; Goodwin 1997; Boily & Kroupa 2003b; Baumgardt & Kroupa 2007; Bastian & Goodwin 2006; Goodwin & Bastian 2006).

In a large set of simulations, Baumgardt & Kroupa (2007) studied the dispersal of the residual gas by decreasing the mass with different star formation efficiency (SFE), and in different tidal fields. They concluded that the clusters had to form with $\text{SFE} \geq 30\%$ in order to survive gas expulsion, and the external tidal fields have significant influences only if the ratio of half mass radius to tidal radius is larger than 0.05. Goodwin & Bastian (2006) and Bastian & Goodwin (2006) addressed a similar problem and found that the embedded clusters would be destroyed within a few tens of Myr if the “effective star formation efficiency” (hereafter eSFE) $\leq 30\%$.

Chen & Ko (2008) studied the behavior of embedded clusters when the parent cloud is dispersing (i.e., the size increases but the total mass remains constant, thus the cloud becomes more and more diluted). From a large survey of simulations we found that the final structure can be classified, according to the expansion ratio of r_{45} (the 45% Lagrangian radius of the cluster), into three groups: (i) destroyed, (ii) loose structure, and (iii) compact core. Empirically, the expansion ratio is related to the cluster-cloud mass ratio (which will be defined later in this paper).

In this work, we address the problem of what determines the fate of the embedded cluster. We consider that the cluster and the parent cloud could have different initial density profiles. Hence we examine three parameters of the parent cloud independently: (i) mass, (ii) size, and (iii) dispersing rate of the cloud. Clusters with and without mass functions are considered. The paper is organized as follows. In Section 2, we describe the model and simulations. In Section 3, we discuss the applicability of SFE as an indicator for describing

the behavior of the cluster, and then introduce other better indicators for more general initial conditions. A summary and some remarks are provided in Section 4.

2. Model

To study the survivability of embedded star clusters, we consider an idealized model. We put a spherical star cluster at the center of an expanding spherical molecular cloud, and then examine the subsequent behavior numerically. In our simulations, the distribution of stars in the cluster is Plummer (1911) with a length scale of 0.6 pc (note that the half mass radius is ~ 0.8 pc). The cloud is represented by an external Plummer (1911) potential in which the length scale increases with time to represent the dispersion of a cloud. We adopt the N -body simulation code *NBODY2* (Aarseth 2001) to study the evolution of the clusters.

Similar systematic simulations have been performed by, e.g., Geyer & Burkert (2001) and Baumgardt & Kroupa (2007). Geyer & Burkert (2001) used the King (1966) model to describe both the cloud and gas, and Baumgardt & Kroupa (2007) used the Plummer (1911) model. Both papers considered equal-mass stars and represented the cloud dispersion as a continuous reduction of cloud mass. In contrast, we mimic cloud dispersion as the expansion of the cloud and the cloud mass does not change.

2.1. Initial condition

We assume that each embedded cluster contains 2500 stars with a total mass of $2500 M_{\odot}$. The physical distribution is Plummer and the length scale, a_c , is about 0.6 pc. The velocity distribution depends on the potential of the parent cloud. The initial mass function (IMF) with Salpeter (1955) slope from 0.3 to $30 M_{\odot}$ is also considered, and there is no primordial mass segregation. All clusters, with the parent clouds, are required to be in virial equilibrium prior to cloud dispersion.

The SFE (and more precisely, the total SFE) is defined as

$$\eta = \frac{M_c}{M_c + M_b}, \quad (1)$$

where M_c is the mass of the cluster and M_b is the mass of the parent cloud. In our runs M_b ranges from 0.5 to $19 M_c$, which gives η from 67% to 5%.

Goodwin (2008) also discussed cases of a cluster and cloud with different spatial distributions but the cluster is in virial equilibrium initially. This is very similar to how we set up

our initial conditions. Note that the eSFE of Goodwin (2008) is related to the length scale of the cloud. More discussion on eSFE will come later.

2.2. Cloud dispersion

The cloud is represented by an external Plummer potential,

$$\Phi_P = \frac{-GM_b}{\sqrt{r^2 + a^2}}, \quad (2)$$

where G is the gravitational constant, r is the distance from the cloud center (which is also the star cluster center), and a is the length scale of the potential. To mimic expansion, we let a increase with time,

$$a = a_0 e^{t/t_e}, \quad (3)$$

where a_0 is the initial length scale and t_e is the dispersing e-fold timescale. A molecular cloud has a relatively short lifetime ranging from a few to a few tens of Myr. We try four different e-fold timescales: from 0.33 to 3.3 Myr. The potential becomes ineffective in no more than two e-fold times (largest dispersing timescale) to 10 e-fold times (smallest dispersing timescale), which corresponds to 7-3 Myr. As molecular clouds are not expected to last longer than 30 Myr, we stop our simulations at 30 Myr after the cloud starts dispersing. In any case, the influence of the gas removal is long gone well before the end of the simulations.

3. Results and discussion

We assume that the embedded clusters are bound and in virial equilibrium initially. When the cloud disperses, the cluster starts to expand. It may be destroyed or may shrink back later by self gravity.

3.1. Cluster and cloud have the same initial density profile

In this subsection, we present some cases for clouds having the same Plummer length scale as the clusters do, 0.6 pc. In these cases, SFE is a good indicator for the subsequent behavior of the clusters. Figure 1 shows the half mass radius (r_{hm}) evolution in different SFEs with a cloud dispersing (or gas removal) timescale of 1.1 Myr. r_{hm} increases almost linearly when SFE is less than 20%. Clusters are destroyed in these cases. For cases with SFE from 25% to 50%, r_{hm} expands slower and shrinks back (even becomes stable) later.

In these runs, clusters remain intact but with different concentrations. The expansion of a cluster by gas removal and then shrinking (collapse) to equilibrium later was also reported in the simulations by Goodwin & Bastian (2006) and Baumgardt & Kroupa (2007), and has also been compared with observations by Bastian et al. (2008).

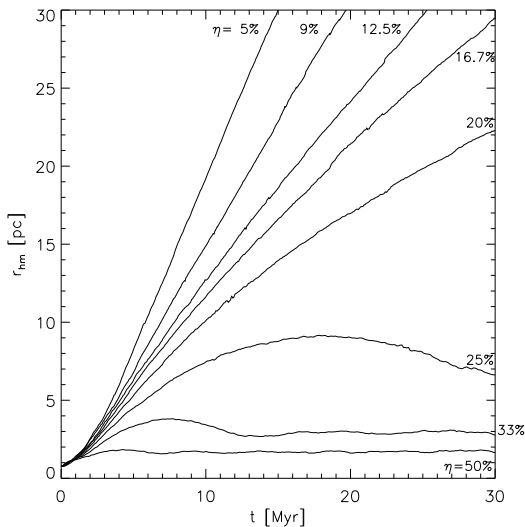


Fig. 1.— Evolution of half-mass radius as a function of time. Here, the dispersing timescale t_e is 1.1 Myr, SFE is from 5% to 50%.

3.1.1. Different dispersing timescales

The behavior is expected to be different if we change the cloud dispersing timescale (or gas removal timescale). Figure 2 shows the r_{hm} evolution of SFE = 25% with four dispersing timescales. r_{hm} increases almost linearly when t_e is 0.33 Myr, and increases slower when t_e is 0.65 Myr. For t_e equal to 1.1 and 3.3 Myr, r_{hm} increases much more slowly and changes little after some time.

3.1.2. Expansion ratio of r_{hm} and bound mass fraction

After dispersing, all clusters expand. To compare the structure before and after, we define the expansion ratio of the half-mass radius r_{hm} as

$$\epsilon = \frac{r_{hm}(\text{final})}{r_{hm}(\text{initial})}. \quad (4)$$

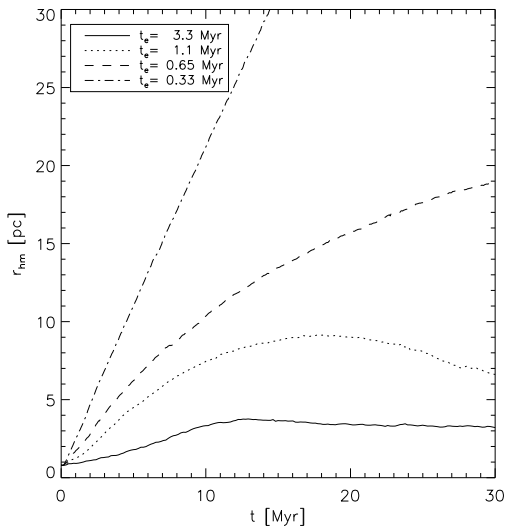


Fig. 2.— Evolution of half-mass radius as a function of time, in terms of Myr. The dispersing timescale here is from 0.33 to 3.3 Myr. The SFE is 25%.

Here final means 30 Myr.

Figure 3 represents the results for the expansion ratio of r_{hm} at the end of the simulations, 30 Myr, as a function of SFE in different dispersing timescales. Different dispersing timescales produce different expansion ratios for the same SFE. For each dispersing timescale, there is a simple relation between η and ϵ . Each relation has two branches joined by a turnover point. Specifically, the turnover points for $t_e = 3.3, 1.1, 0.65, 0.33$ Myr are at $\eta \approx 0.18, 0.25, 0.33, 0.50$, respectively. The steeper branch corresponds to destroyed clusters and the flatter branch to survived clusters. Hence the SFE, η , is a good indicator for the survivability of embedded clusters.

Figure 4 depicts the bound mass fraction as a function of SFE in different dispersing timescales (or gas removal timescale). Both Figures 3 and 4 nicely demonstrate the expected result: a cluster might survive in a slowly dispersing cloud but might be destroyed in a fast dispersing one. The dependence of the bound mass fraction on SFE is also reported by Baumgardt & Kroupa (2007). Based on this relation, Parmentier et al. (2008) discussed the shape of the initial cluster mass function.

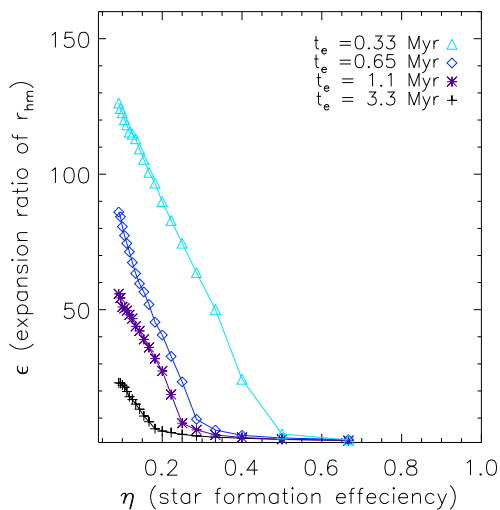


Fig. 3.— Expansion ratio of half-mass radius as a function of SFE. (A color version of this figure is available in the online journal.)

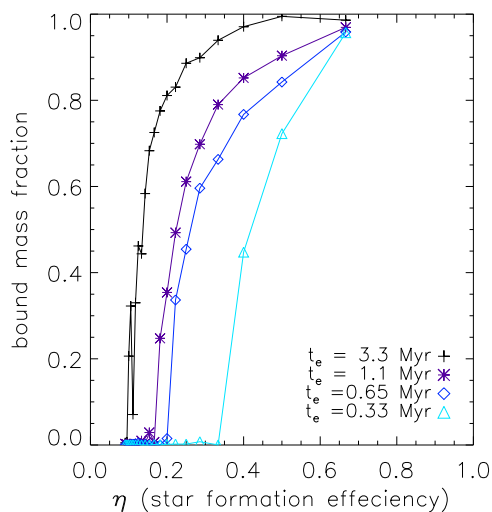


Fig. 4.— Bound mass fraction as a function of SFE. (A color version of this figure is available in the online journal.)

3.2. Cluster and cloud have different initial density profiles

We suppose that it is too idealized to consider both cluster and cloud have the same initial density profile (as in the previous section), and it is conceivable that they are more likely to have different initial profiles. To study the cases with different initial profiles, we fixed the Plummer length scale of the cluster at 0.6 pc, but varied the Plummer length scale of the cloud from four times smaller to four times larger than that of the cluster. Thus, there are two parameters to describe the initial profile of the cloud: $\{M_b, a_0\}$, its mass and the initial Plummer length scale. (One can use the SFE η and a_0 instead.) It is obvious that η alone is not sufficient to describe the results with different a_0 and M_b (or equivalently η , see Equation (1)). When we plot the expansion ratio ϵ of 20 a_0 cases against η (see Figure 5), no discernible relation(s) can be found. (We should point out that if we plot the result of one a_0 , the graph will be similar to Figure 3.)

However, ϵ does show a “simple relation” with $\{M_b, a_0\}$. Figure 6 shows the contours of ϵ in the parameter space $\{M_b, a_0\}$ for the dispersing timescale $t_e = 3.3$ Myr. Understandably, ϵ is large/small (cluster is destroyed/remains intact) when a_0 is small/large and M_b is large/small (or η is small/large). In fact, there are three final configurations for the cluster: (i) destroyed, (ii) loose structure, and (iii) compact core. The boundaries between these configurations closely match the contours $\epsilon = 10$ and 2 for the cases with different dispersing rates (for details, see Chen & Ko 2008). In other words, on the one hand for a fixed effective size of the natal cloud, it is clear that the survivability of the cluster is higher when the SFE is larger. On the other hand, for a fixed SFE, the survivability increases when the effective size of the natal cloud increases. For example, when the cloud contains 90% of the mass of the system (i.e., total SFE 10%), the half-mass radius of the cluster expands at least twice in 30 Myr. The smaller the size of natal cloud, the more the star cluster will expand. Apparently, the reason is the dynamics of the cluster is dominated more by the cloud when the mass of cloud initially enclosed within the cluster is more, such as the cases of small SFE and small effective natal cloud size. And in contrast for the cases of large SFE and large effective natal cloud size, the dynamics is dominated by the cluster.

Although SFE η fails to be a good survivability indicator of the two-parameter system, we are able to identify other survivability indicators: the initial cluster-cloud mass ratio and the initial kinetic energy. We describe these two indicators in the following separately.

Cluster-cloud mass ratio

First denote the mass fraction f Lagrangian radius of the cluster as r_f , i.e., within r_f the mass of the cluster is fM_c , and denote this mass by $M_{c,r_f} = fM_c$. Also denote M_{b,r_f} as the

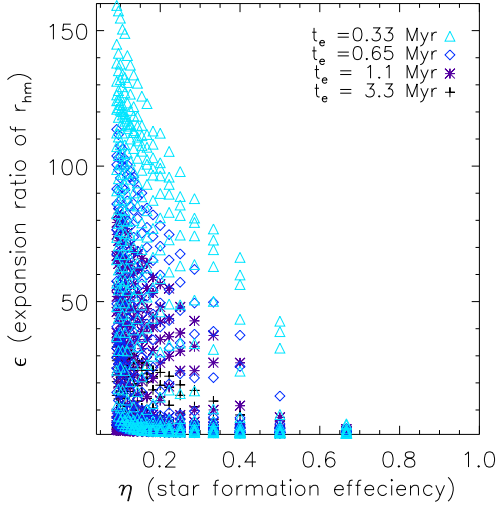


Fig. 5.— A plot of the expansion ratio of half-mass radius against SFE for 20 cases of a_0 . (A color version of this figure is available in the online journal.)

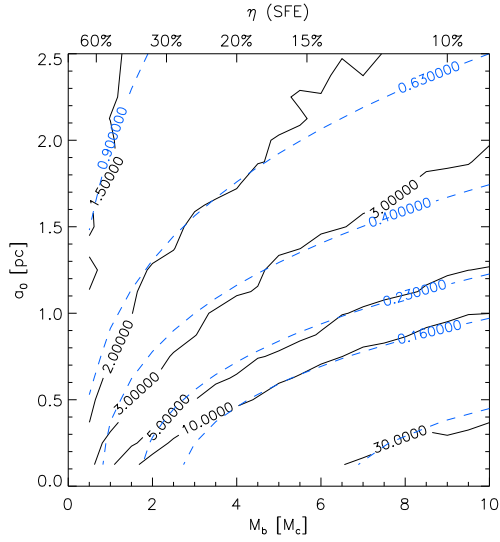


Fig. 6.— Contours of the expansion ratio of half-mass radius ($\epsilon_{r_{hm}} = \epsilon_{r_{50}}$, solid line) in the parameter space $\{M_b, a_0\}$. The dashed lines are contours of the cluster-cloud mass ratio at half-mass radius, $\beta_{r_{hm}} = \beta_{r_{50}}$. In this example, the cloud dispersing timescale is $t_e = 3.3$ Myr. The corresponding SFE is labeled at the top. (A color version of this figure is available in the online journal.)

mass of the cloud within r_f initially. Define the cluster-cloud mass ratio as (see Chen & Ko 2008)

$$\beta_{r_f} = \frac{M_{c,r_f}}{M_{c,r_f} + M_{b,r_f}}. \quad (5)$$

This closely resembles the definition of SFE η (see Equation (1)), but β_{r_f} contains information about the length scale of the cloud a_0 . Note that $\beta_\infty = \eta$ (when $f = 1$, $r_f \rightarrow \infty$). Since we are using the Plummer model for both cluster and cloud, there is a simple relation between β_{r_f} and η

$$\left(\frac{1}{\eta} - 1\right) = \frac{f}{F} \left(\frac{1}{\beta_{r_f}} - 1\right), \quad (6)$$

where $f = M_{c,r_f}/M_c$ and $F = M_{b,r_f}/M_b = r_f^3/(r_f^2 + a_0^2)^{3/2}$. We also extend the half-mass radius expansion ratio of Equation (4) to

$$\epsilon_{r_f} = \frac{r_f(\text{final})}{r_f(\text{initial})}. \quad (7)$$

We find that for each dispersing timescale t_e , f can be tuned such that data from the two-dimensional parameter space $\{M_b, a_0\}$ collapses to a relation in the $\beta_{r_f} - \epsilon_{r_f}$ plane, see Figure 7. The relation closely resembles the relation $\eta - \epsilon$ for cases of fixed a_0 (compared to Figures 7 and 5) and the turnover points for $t_e = 3.3, 1.1, 0.65, 0.33$ Myr are at $\beta_{r_f} \approx 0.18, 0.28, 0.40, 0.53$, respectively. We note that r_f does not increase monotonically with increasing dispersion timescale.

We stress that although it may seem a bit contrived that we have to tune r_f to obtain a tight relation, the result is reasonably good even if we pick one particular r_f for all timescales. Figure 8 shows the relations at half-mass radius for all dispersing timescales (i.e., $\epsilon_{r_{hm}}$ against $\beta_{r_{hm}}$). In Figure 6, we see that the contours of $\epsilon_{r_{hm}}$ and $\beta_{r_{hm}}$ agree with each other in the parameter space $\{M_b, a_0\}$.

Initial kinetic energy or virial energy

To clarify the relation between the final state and the initial condition, we also check the energies. We find that the initial kinetic energy is nicely correlated with the expansion ratio of half-mass radius ϵ , see Figure 9. Since the initial system is in virial equilibrium, the initial virial energy is just twice of the kinetic energy, hence it should also be a good indicator.

The initial kinetic energy and the initial virial energy show how the cloud mass affect stars inside the cluster. β_{r_f} is the cluster-cloud mass ratio within a certain region. All of them show nice relations with the expansion ratio ϵ or ϵ_{r_f} . But if one would like to apply to

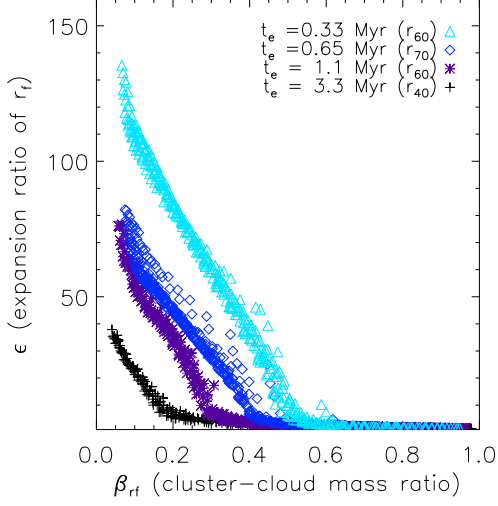


Fig. 7.— Expansion ratio of the chosen Lagrangian radii as a function of the cluster-cloud mass, β_{r_f} . (A color version of this figure is available in the online journal.)

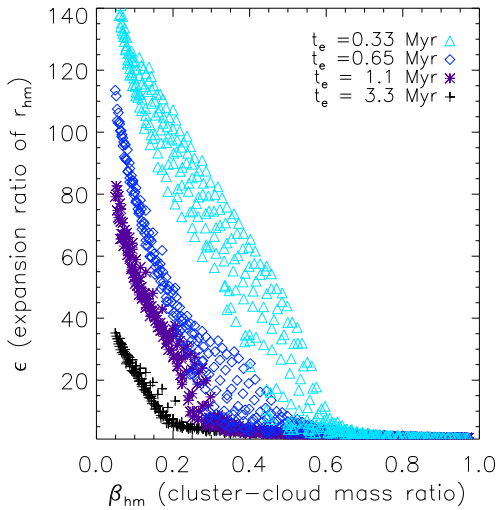


Fig. 8.— Expansion ratio of the half-mass radius as a function of the cluster-cloud mass, β_{r_f} . Here f is 0.5. (A color version of this figure is available in the online journal.)

observations, it might not be easy to obtain the energy estimation for the whole cluster. β_{r_f} should be the more convenient choice.

Figure 10 shows three initial mass density profiles of clusters and clouds at a particular cloud mass M_b/M_c or total SFE η . In the figure, $M_b/M_c = 4$ and $\eta = 0.2$. The upper panels show the density profiles against radius and the lower panels show the corresponding β_r against radius. Note that $\beta_r \rightarrow \eta$ as $r \rightarrow \infty$. In the middle column, $a_0 = a_c$, the two density distributions are the same, and the corresponding β_r is always 0.2 at any radius. In the left column, $a_0 < a_c$ (i.e., comparatively the cloud mass is distributed more concentrated at the origin than the cluster), β_r increases monotonically with r (from $\beta_r < \eta$ towards η as $r \rightarrow \infty$ and β_r always smaller than η). In the right column, $a_0 > a_c$ (i.e., comparatively the cloud mass is distributed more evenly than the cluster), β_r decreases monotonically with r (from $\beta_r > \eta$ towards η as $r \rightarrow \infty$ and β_r always larger than η). Therefore, for every total SFE, we have three distinct types: $a_0 <, =, > a_c$. The cluster has a higher/lower chance to survive when the cloud size is larger/smaller than the cluster size at a given total SFE. This also suggested that at a low total SFE the cluster has a higher chance to survive if the length scale of cloud is larger.

To this end, we would like to point out a similar idea introduced by Goodwin (2008). The effective SFE, eSFE, is defined as the virial ratio of the stars after instantaneous gas expulsion. The total SFE equals the eSFE when the cluster and cloud share the same density profile. When the cluster is born dynamically “cold/hot”, the velocity of a cluster is smaller/larger than what is required for virial equilibrium, the eSFE is larger/smaller and the cluster has a better/worse chance to survive. This is comparable to our results of clouds with larger/smaller length scales.

Moreover, eSFE is closely related to the initial kinetic energy of the cluster that we mentioned earlier. For a fixed total SFE, the initial kinetic energy is smaller if the size of the natal cloud is larger. In this case the cluster is ‘colder’ and tends to survive after the cloud dispersed.

3.3. Mass segregation

Mass segregation is another important issue in stellar clusters. Once again we use NBODY2 to study mass segregation. All simulations start with the Salpeter mass function, i.e., the mass function slope is -1.35 . We find that $\beta_{r_{hm}}$ is also a good indicator for the level of mass segregation. Figure 11 shows the mass function slope derived from within the final half density radius as a function of $\beta_{r_{hm}}$ for cases with $\epsilon_{r_{hm}} \leq 20$. When $\beta_{r_{hm}}$ is small (i.e.,

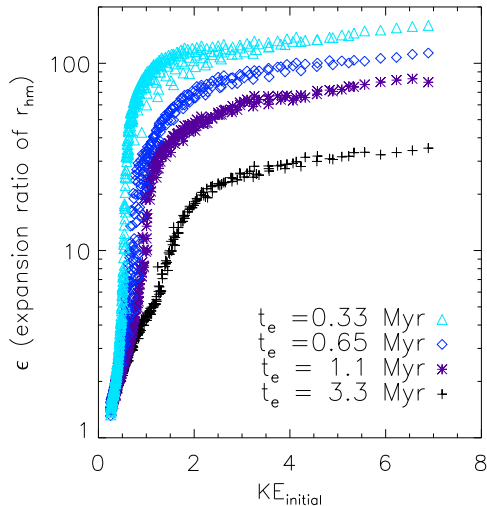


Fig. 9.— Initial kinetic energy and the expansion ratio of half-mass radius. The units of the initial kinetic energy here are in $N - body$ units. (A color version of this figure is available in the online journal.)

cloud mass is the dominant factor), the mass segregation of the cluster is less severe. We note that using different β_{r_f} does not change the relation much.

The preferential loss of low-mass stars is due to two-body relaxation (see Spitzer 1958; Spitzer & Härm 1958) and would flatten the mass function. We should point out that we fit the mass function by a simple single power law, which is not the best fit for all cases. As a matter of fact, the broken power law observed in the Arches cluster (Kim et al. 2006) is also seen in our simulations. We note that this could also be obtained by dynamical evolution without a natal cloud (see also Portegies Zwart et al. 2007). However, we cannot find an obvious relation between the broken power law and SFE η or the cluster-cloud mass ratio β . This may be due to poor statistics in our runs (2500 stars initially). Moreover, the broad distribution of the final mass function slope in Figure 11 is perhaps a result of the simple single power law fitting.

4. Summary and Remarks

We studied the consequence for clusters after parent clouds disperse in different dispersing timescale, cloud mass, initial cloud length scale, and IMF. We mimic cloud dispersal by increasing cloud size or length scale, but keeping the total cloud mass unchanged.

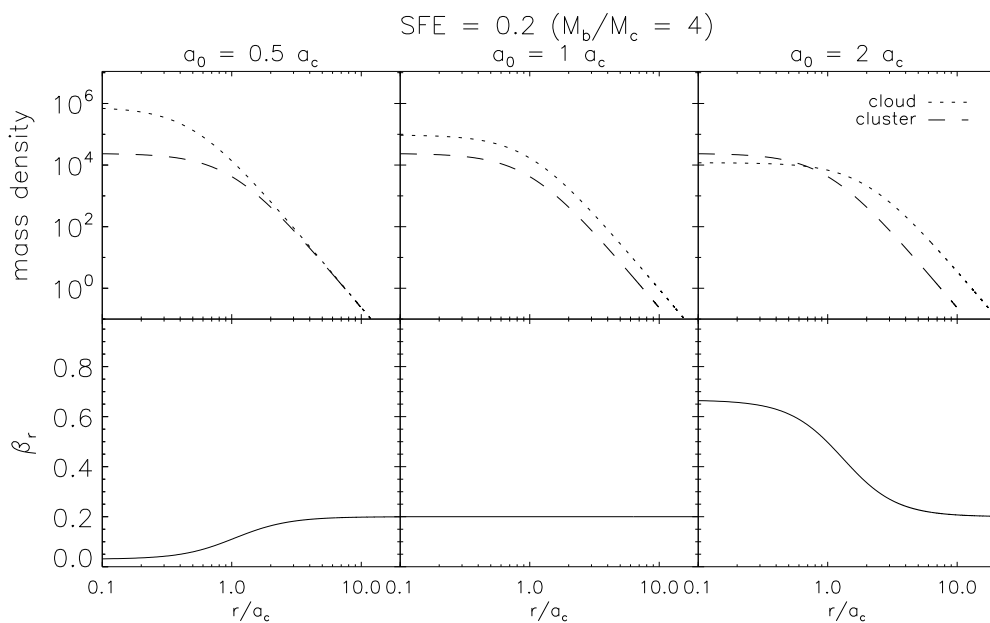


Fig. 10.— Mass density profiles and the corresponding cluster-cloud mass ratio, β_r , for cases with different length scales of the cloud. The total SFE $\eta = 0.2$ (i.e., $M_b/M_c = 4$). From left to right, the ratios of length scale of the cloud to cluster are 0.5, 1, and 2, respectively. The mass of cloud is more concentrated (cloud-dominated) in the left column and more spread out (cluster-dominated) in the right column. The mass densities are in arbitrary units.

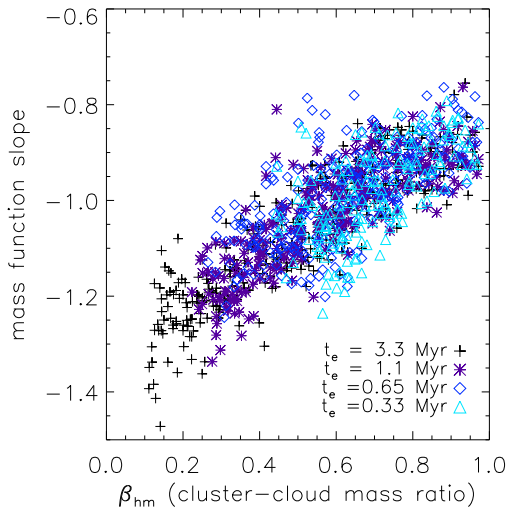


Fig. 11.— Mass function slope as a function of half-mass β value. The mass function slope is derived from stars within the final half-density (2D) radius. The IMF slope is -1.35 (Salpeter) for all cases. (A color version of this figure is available in the online journal.)

SFE, η , is a good indicator for the survivability of embedded cluster after the dispersal of the parent cloud only if the cluster and cloud have the same density profile. It fails badly if the cluster and cloud have different density profiles. The latter cases can be described by two parameters $\{M_b, a_0\}$, the mass of the cloud and the length scale of the Plummer model. The expansion ratio of the cluster is obviously depending on the two parameters. Although we cannot use η as a survival indicator, we find two quantities that can serve the same purpose.

The two quantities are (i) the initial cluster-cloud mass ratio (within a certain Lagrangian radius of the cluster), β_{r_f} (see Equation (5)), and (ii) the initial kinetic energy (or virial energy). Each of them can organize the data of itself and the expansion ratio (of a certain Lagrangian radius of the cluster) at a dispersing timescale into a ‘one-dimensional’ relation (effectively collapsing data from a surface into a line). Moreover, the relation is very nice in the sense that it has two branches, one corresponds to cluster destruction and the other to survival. Hence the two quantities are good indicators for the survivability of embedded clusters.

We should point out that for different cloud dispersing timescales we need to choose somewhat different Lagrangian radius to obtain the tightest correlation between the cluster-cloud mass ratio and the expansion ratio. Having said that, in fact, $\beta_{r_{hm}}$ fits the data rea-

sonably well for all different cloud dispersion rates . The tight correlation strongly suggested that the evolution of the embedded cluster depends on the total mass enclosed within the corresponding Lagrangian radius of the cluster. We thus propose that the relevant (initial) effective timescales should be defined in terms of the total mass enclosed within the best-fit Lagrangian radius (or roughly the half-mass radius where $f = 0.5$) (e.g., Binney & Tremaine 1987),

$$\tau_{\text{relax}} \approx \frac{fN}{8\beta_{r_f}^2 \log(fN/\beta_{r_f})} \tau_{\text{cross}}, \quad \tau_{\text{cross}} \approx \sqrt{\frac{\beta_{r_f} r_f^3}{fGM_c}}, \quad (8)$$

where N is the number of stars in the cluster, and τ_{relax} and τ_{cross} are, respectively, the effective relaxation time and crossing time.

Furthermore, for clusters with Salpeter mass function, the slope of the final mass function shows a roughly linear relation with the cluster-cloud mass ratio at half-mass radius, $\beta_{r_{hm}}$, see Figure 11. In addition, all the dispersing rates we considered share the same relation.

As mentioned in Section 2, similar works have been done with an equal-mass model (e.g., Geyer & Burkert 2001; Baumgardt & Kroupa 2007). Goodwin (1997) mentioned that the survivability of the clusters is only slightly higher in the cases of equal mass than cases with mass function. For comparison with the result of mass function presented here, we also did the same simulation survey for the cases of equal mass. We confirm that there is no significant difference on the total mass of escaping stars. However, the mass distributions would be different for radii larger than r_{70} (70% Lagrangian radius) in these two models.

Observationally, the initial kinetic energy of the whole star cluster is not easy to estimate. On the other hand, the cluster-cloud mass ratio is more promising and should warrant further studies.

We thank the referee for valuable suggestions to an earlier version of the paper. This work was supported in part by the National Science Council, Taiwan under the grants NSC-96-2112-M-008-014-MY3.

REFERENCES

- Aarseth S.J., 2001, *New Astronomy*, 6, 277
 Baumgardt H., Kroupa P., 2007, *MNRAS*, 380, 1589

- Bastian N., Gieles M., Goodwin S. P., Tranco G., Smith L. J., Konstantopoulos I., Efremov Yu., 2008, MNRAS, 389, 223
- Bastian N., Goodwin S.P., 2006, MNRAS, 369, L9
- Binney J., Tremaine S., 1987, Galactic Dynamics (Princeton, NJ : Princeton Univ. Press)
- Blitz L., Shu F., 1980, ApJ, 238, 148
- Boily C.M., Kroupa P., 2003a, MNRAS, 338, 665
- Boily C.M., Kroupa P., 2003b, MNRAS, 338, 673
- Bonnell I. A., Dobbs C. L., Robitaille T. P., Pringle J.E., 2006, MNRAS, 365, 37
- Chen H.-C., Ko C.-M., 2008, Astron. Nachr., 329, 1053
- Elmegreen B., 2000, ApJ, 530, 277
- Gieles M., Portegies Zwart S.F., Baumgardt H., Athanassoula E., Lamers H.J.G.L.M., Sipior M., Leenaarts J., 2006, MNRAS, 371, 793
- Geyer M. P., Burkert A., 2001, MNRAS, 323, 988
- Goodwin S.P., 1997, MNRAS, 284, 785
- Goodwin S.P., 2008, to appear in the proceedings of the meeting, “Young massive star clusters - Initial conditions and environment”, ed. E. Perez et al., Granada, Spain, September 2007 (Springer: Dordrecht)
- Goodwin S.P., Bastian N., 2006, MNRAS, 373, 752
- Hartmann L., Balesteros-Paredes J., Bergin E. A., 2001, ApJ, 562, 852
- King I. R., 1966 AJ, 71,64
- Kim S. S., Figer D. F., Kudritzki R. P., Najarro F., 2006, ApJ, 653, L113
- Lada C.J., Lada, E.A. 2003, ARA&A, 41, 57
- Lada C.J., Margulis M., Dearborn D., 1984, ApJ, 285, 141
- Leisawitz D., Bash F. N., Thaddeus P. 1989, ApJS, 70, 731
- Parmentier G., Goodwin S. P., Kroupa P. and Baumgardt H., 2008, ApJ, 678, 347

Plummer H. C., 1911, MNRAS, 71, 460

Portegies Zwart S., Gaburov E., Chen H.-C., Gürkan M. A., 2007, MNRAS, 378, 29

Salpeter E.E., 1955, ApJ, 121, 161

Spitzer L., 1958, ApJ, 127, 544

Spitzer L., Härm R., 1958, 127, 17.

Tutukov A. V., 1978, A&A 70, 57

Williams J., McKee C.F., 1997, ApJ, 476, 166